

Excitation and detection schemes in pulsed EPR

Arthur Schweiger

Laboratorium für Physikalische Chemie, Eidgenössische Technische Hochschule,
8092 Zürich, Switzerland

Abstract

The paper describes a number of pulsed EPR techniques for investigating the structure of paramagnetic compounds. The survey is divided in three parts: (a) *Echo detection*: – Remote echo detection, – Four-pulse ESEEM, – soft ESEEM, – rf-driven ESEEM, – ESEEM with improved modulation depth; (b) *FID-detected hole burning*: – FT-ESR detected NMR, – FT-hyperfine spectroscopy, – Electron-Zeeman-resolved EPR, – Orientation-selective EPR; (c) *Continuous-wave detection*: – Inversion-recovery detected EPR, – Electron spin transient nutation spectroscopy.

INTRODUCTION

Pulsed EPR spectroscopy has now come of age. It is a field of research which has emerged from its former shadowy existence and is undergoing extraordinarily rapid development (ref.1–3). In this contribution various new pulsed EPR methods recently developed in our laboratory will be discussed. The first class of experiments deals with the nuclear modulation effect. Several pulse schemes have been introduced for improving resolution and sensitivity and overcoming instrumental distortions. A second class of experiments is based on a novel detection scheme: FID-detected hole burning. It will be demonstrated that this approach not only improves some of the standard techniques using echo detection, but also offers new possibilities for the elucidation of magnetic parameters. Finally, cw-detected pulsed EPR is proposed. This detection scheme is particularly useful for the measurement of electron spin transient nutations in spectra with inhomogeneously broadened lines.

ECHO-DETECTION

The standard two- and three-pulse ESEEM experiments suffer from several disadvantages: The instrumental deadtime τ_d prevents the observation of broad hyperfine lines; the strong zero frequency component is often difficult to eliminate; the modulation amplitudes (determined by the magnetic parameters) may be below the detection limit; blind spots in three-pulse ESEEM complicate the interpretation of the data; the excitation of allowed and forbidden transitions requires strong mw pulses; the stepwise measurement of the echo envelope is time consuming.

Based on echo detection, a number of new pulsed EPR schemes has recently been introduced to avoid these drawbacks and to improve the potentiality of the ESEEM experiment.

1. Remote echo detection

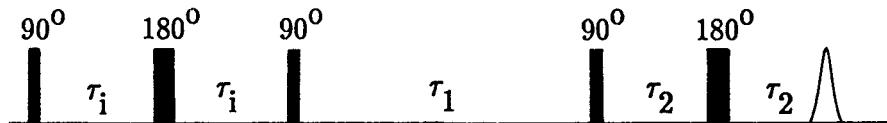


Fig.1: Pulse sequence for remote echo detection

In an electron spin echo experiment instrumental deadtime artifacts may efficiently be eliminated using remote echo detection (ref.4). In this approach the first two pulses, separated by the interval τ_i , generate the usual two-pulse echo at a time τ_i after the 180° pulse (Fig.1). However, in contrast to the standard procedure this short-lived transverse magnetization is not recorded, but is instead converted into longitudinal magnetization by a further 90° pulse, and "stored" for a time interval of the order of T_1 . After a fixed delay

time $\tau_1 < T_1$ the stored z-magnetization can be "read out" by means of a further two-pulse experiment with a pulse interval $\tau_2 > \tau_d$.

Increasing τ_1 in a series of steps gives an ESEEM pattern which corresponds to the usual two-pulse echo modulation, but with the important difference that the deadtime after the first two pulses no longer effects the echo amplitude data. A similar adaptation of the stimulated echo ESEEM is straight forward.

2. ESEEM with improved modulation depth

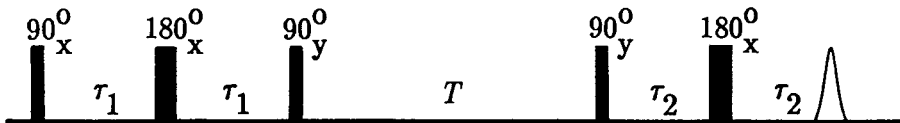


Fig.2: Sequence of the five-pulse ESEEM experiment with improved modulation depth

In the three-pulse ESEEM experiment the first two pulses produce nuclear spin coherence, which then evolves during the evolution time T , and is converted by the third pulse into observable electron spin coherence. This transfer of coherence, however, is not optimum. An improved coherence transfer is obtained, for example, with a five-pulse sequence (Fig.2), in which the first three pulses with a fixed time interval τ_1 produce nuclear spin coherence (ref.5). The nuclear spin coherence is maximized if the phase of the third pulse is shifted by 90° relative to that of the first two pulses. After a variable evolution time T the nuclear spin coherence is measured via a two-pulse echo sequence.

With this sequence it is theoretically possible, in the case of a small modulation depth parameter to obtain a modulation amplitude up to eight times greater than in the three-pulse experiment, while at the same time keeping the unmodulated component of the echo intensity close to zero.

3. Soft ESEEM

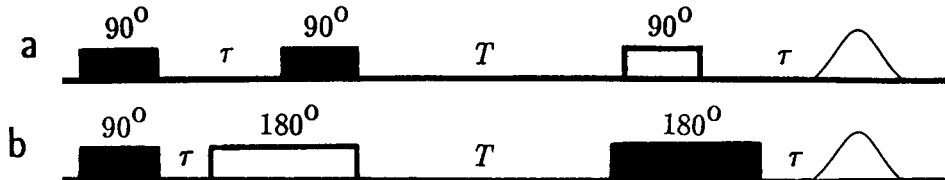


Fig.3: Soft ESEEM sequences, a) primary soft ESEEM, b) stimulated soft ESEEM

In the conventional two- and three-pulse ESEEM experiment, both allowed and forbidden electron spin transitions have to be excited simultaneously. This requires hard (short and strong) mw pulses and correspondingly high mw field strengths.

In the soft ESEEM approach, allowed and forbidden transitions are excited separately by soft (long and weak) pulses with two different mw frequencies. Both, a primary (ref.6) and a stimulated (ref.7) soft ESEEM experiment has been proposed. The primary soft ESEEM sequence (Fig.3a) consists of three selective 90° pulses. The first pulse creates electron spin coherence which evolves during the variable time τ and is then stored as spin polarization during the fixed time T . The third pulse converts the polarization back to electron spin coherence which is detected as an echo. In this experiment the echo decays with T_{2e} .

The stimulated soft ESEEM sequence (Fig.3b) is based on the transfer of coherence from the electron to the nuclei and then back to the electron spin transitions. With this pulse sequence, τ is fixed and T varied. During the time period T after the second pulse, the nuclear spin coherence decays with T_{1e} . Since T_{1e} is typically much greater than T_{2e} , the echo modulation is observable for a longer period of time resulting in greater spectral resolution.

The soft ESEEM method has several advantages compared with the standard ESEEM schemes. The experiment can be performed with a mw power level two to three orders of magnitude smaller than that for an experiment with hard pulses. Also the soft ESEEM method makes it possible to observe modulation frequencies well above 100 MHz.

4. Sum-frequency spectrum in four-pulse experiments

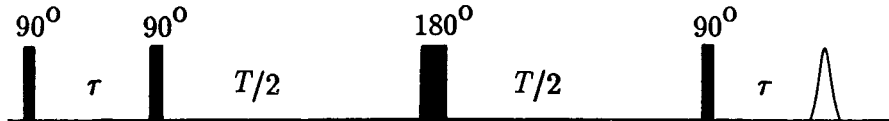


Fig.4: Four-pulse sequence for the measurement of highly resolved sum-peak spectra

In two-pulse experiments one observes, for each $I=1/2$ nucleus, not only the fundamental frequencies ω_α and ω_β but also the sum frequency $\omega_\alpha + \omega_\beta$. Because of the partial refocussing of the hyperfine interactions, the sum peaks appear as narrow lines in the neighborhood of $2\omega_I$, i.e. twice the nuclear Zeeman frequency.

In a disordered system the sum peaks extend over the frequency range from $2\omega_I$ to ω_{\max} . The frequency shifts $\Delta = \omega_{\max} - 2\omega_I$ are closely related to the dipolar parts of the hyperfine couplings and contain important information about the positions of the nuclei (ref.3,8,9).

In most cases the widths of the individual sum-frequency peaks are determined by the short phase memory time. To improve the spectral resolution a pulse sequence which allows nuclear spin coherence to evolve during a variable time interval has to be used. If in a three-pulse ESEEM sequence a nonselective 180° pulse is inserted at a time $T/2$ after the second 90° pulse (Fig.4) and T is increased in a stepwise manner, sum frequencies again appear (ref.10). The slow decay of the echo intensity during the evolution time T results in a greatly improved resolution of the sum-frequency peaks (ref.11).

5. RF-driven ESEEM

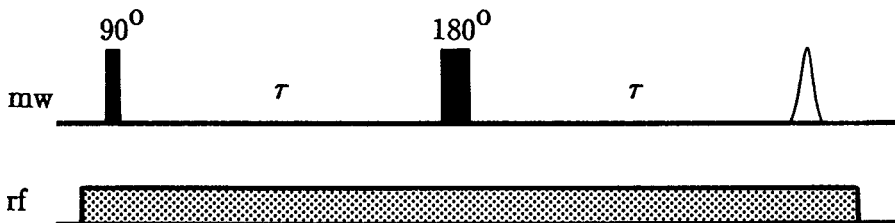


Fig.5: Pulse sequence of the rf-driven ESEEM experiment

The requirement that nonsecular terms be present in the spin Hamiltonian excludes several important categories of paramagnetic systems as candidates for ESEEM studies. Radicals in solution are perhaps the most prominent of these. In such systems echo modulations may be created by combining pulsed irradiation of the sample by mw fields with continuous irradiation by an rf field during the entire pulse sequence (Fig.5). Since the echo modulation is actually effected by the rf irradiation, the method is called "rf-driven ESEEM" (ref.12). The observed frequencies can easily be related to the isotropic hyperfine coupling constants. In addition, the modulation patterns are indicative of the number of magnetically equivalent nuclei coupled to the unpaired electron.

FID-DETECTED HOLE BURNING

In an FID-detected hole burning experiment, a soft preparation pulse burns a narrow hole into the inhomogeneously broadened EPR line. Then, a perturbation is applied that shifts the hole or transfers part of the hole to a new position in the EPR line. The perturbation can be represented by an rf field pulse, an electric or magnetic field that is turned on, a rotation of the sample around an axis perpendicular to B_0 , etc. The new position of the hole is measured via an FID, induced by a nonselective 90° pulse.

The soft preparation pulse followed by the hard detection pulse represents a special type of a stimulated echo sequence. In a standard stimulated echo experiment, the two first nonselective 90° pulses create a periodic polarization or hole pattern (Fig.6) which is represented in the time domain by a signal at $t=0$ and a feature at time τ (called echo).

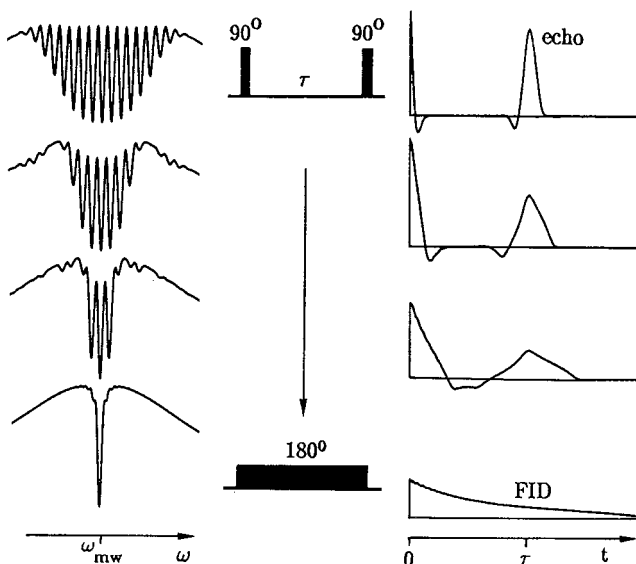


Fig. 6:

Polarization patterns of a $S=1/2$ spin system for different preparation sequences (left) and corresponding transient signals (right) that follow a nonselective 90° pulse.

Going gradually from this two-pulse sequence to a soft 180° pulse, one ends up with a narrow hole in the EPR line and a corresponding extended transient signal (called FID).

Whenever a pulsed EPR experiments demands for a high B_0 field selectivity, FID-detected hole burning is superior to echo detection.

1. FT-EPR detected NMR



Fig. 7: Pulse sequence of FT-EPR detected NMR

FT-EPR detected NMR is an alternative to ESEEM for the determination of nuclear transition frequencies (ref.13). The approach is based on the driving of forbidden transitions by a selective Gaussian shaped mw pulse followed by the detection of the created holes via an FID. The main advantage of FT-EPR detected NMR as compared to ESEEM is its higher sensitivity. This is based on two effects: (i) In FT-EPR detected NMR the forbidden transitions in spin systems with small nonsecular terms can be driven strongly and selectively for optimum signal intensity (with nominal flip angles of up to several thousand degrees), whereas in the standard two- and three-pulse ESEEM experiment, the modulation depth is fully determined by the Hamiltonian and thus may not be changed in a simple way by experimental manipulations. (ii) The FT-EPR detected NMR signal, which contains all the information about the nuclear transition frequencies can be recorded in a single experiment, whereas in an ESEEM approach the modulation pattern has to be measured step by step.

Apart from the sensitivity argument, FT-EPR detected NMR has the advantage that blind spots as well as sum and difference frequencies do not appear. Moreover, the interpretation of the spectra is simplified by the fact that the transition frequencies of each nucleus have the same relative signal intensity and that this intensity can be changed at will, just by varying the flip angle of the selective mw preparation pulse.

2. FT-hyperfine spectroscopy

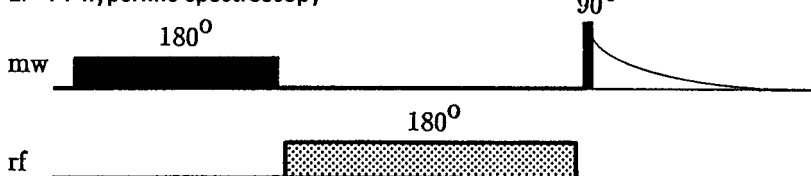


Fig. 8: Pulse sequence of FT-hyperfine spectroscopy

In this hole burning experiment (Fig.8) a selective mw 180° pulse on-resonance with one of the allowed EPR transitions burns a (center) hole into the EPR line. The rf 180° pulse on-resonance with one of the nuclear transition frequencies transfers part of this hole to

side holes shifted from the center hole by the *hyperfine splitting* (ref.14). The resulting hole pattern is again detected via an FID. In the corresponding FT-hyperfine spectrum, each class of equivalent nuclei is then represented by *one* peak, independent on the nuclear spin quantum number.

FT-hyperfine spectroscopy is a powerful method for the identification of lines in crowded ENDOR spectra of systems, where the hyperfine splitting is smaller than the inhomogeneous linewidth. In this approach the ENDOR spectrum is disentangled into a second dimension, the hyperfine dimension. In the 2D representation of the experiment, each peak is then characterized by an ENDOR frequency and by a hyperfine splitting.

3. Electron-Zeeman-resolved EPR

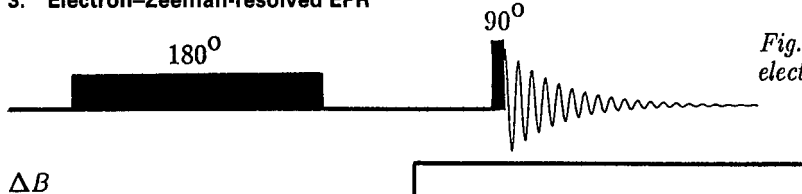


Fig.9: Pulse sequence used in electron-Zeeman-resolved EPR

Electron-Zeeman-resolved EPR is based on the g-value dependence of the electron Zeeman interaction, and allows one to expand a field-swept EPR spectrum in a second dimension, representing the electron-Zeeman frequency (ref.15). A selective mw 180° pulse again burns a hole into the inhomogeneously broadened EPR line. After this pulse, the magnetic field strength is changed from B_0 to $B_0 + \Delta B$. This causes a shift of the EPR line (including the hole) by $\Omega = (g\beta_e/\hbar)\Delta B$, which is measured using FID-detection. Repetition of the experiment for a set of B_0 values results in a 2D EPR spectrum $S(B_0, \Omega)$ with peaks at $B_0 = (\hbar/g\beta_e)(\omega_{mw} - m_J a)$, $\Omega = (g\beta_e/\hbar)\Delta B$.

The approach is useful to disentangle overlapping single crystal spectra, and to separate different orientations in a powder spectrum. The method should even be capable of reducing line broadenings due to g strains in spectra of ordered and disordered systems.

4. Orientation-selective EPR

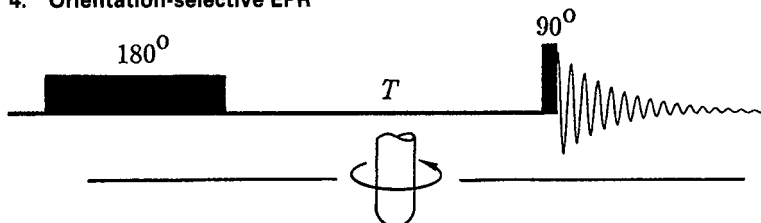


Fig.10: Pulse sequence of orientation-selective EPR

Orientation-selective EPR is based on the orientation dependence of the anisotropic magnetic parameters. During the hole burning sequences the sample is rotated with several hundred Hertz about an axis perpendicular to B_0 (Fig.10). If time T is much larger than the length of the preparation pulse, the influence of the rotation on the hole burning process can be neglected. For spin packets with orientations close to a principal axis of a magnetic interaction tensor, the resonance conditions will not change under sample rotation, e.g. the position of the hole remains the same for these stationary points. However, for all other orientations, the hole will be shifted and the corresponding FID will oscillate.

In the resulting 2D plot, B_0 field versus Ω , where Ω is a measure for the anisotropy defined by $dY/d\theta$ (Y: Electron Zeeman interaction, hyperfine interaction or zero field splitting; θ : rotation angle during time T), the spectral features are much better resolved than in a conventional one-dimensional EPR spectrum.

CW-DETECTION

Up to now we only discussed the detection of transient signals (echoes, FID's) emitted by the sample after pulsed irradiation. An alternative approach to get information about the state of the perturbed spin system is by measuring the response of the spin ensemble under weak continuous mw irradiation (ref.17). In this cw-detection, that follows a sequence of mw pulses, only the on-resonance polarization is recorded.

The most simple pulse sequence consists of a selective mw 180° pulse. Cw-detection then just measures the recovery of the inverted polarization. Figure 11 shows an oscilloscope photograph of inversion recovery signals that follow 180° pulses. This cw-detection scheme offers a new way to record an EPR spectrum: "Inversion recovery—detected EPR".

In such an experiment the recovery of the on-resonance polarization is recorded as a function of B_0 , resulting in an (absorption) EPR spectrum.

1. Electron spin transient nutations



Fig.12: Pulse sequence used in the transition nutation experiment

In a transient nutation (TN) experiment, the TN frequency depends on the magnetic parameters and on the electron spin quantum number. The observation of TN can therefore be used to disentangle complicated EPR spectra (ref.18). Using a modern resonator design (ref.19), TN with frequencies up to 150 MHz are induced by a mw power of 1 kW, resulting in a high resolution along the TN frequency dimension. However, for such high mw powers, the signal may no longer be recorded during excitation.

This problem can be solved by using cw-detection. In such an experiment, the length of the strong mw pulse is increased step by step and the recovery of the *on-resonance polarization* is monitored with a weak cw-probe field (ref.20).

In the 2D representation, TN frequency versus B_0 , the interpretation of single crystal and powder spectra is essentially simplified.

Acknowledgements

Several colleagues have made essential contributions to the research presented in this paper. In particular, I would like to acknowledge the work of Gabi Aebli, Herman Cho, Jörg Forrer, Claudius Gemperle, Eric Hustedt, Remo Jakob, Susanne Pfenninger and Thomas Wacker. Advices of Richard R. Ernst are much appreciated. The research has been supported by the Swiss National Science Foundation.

REFERENCES

1. A.J. Hoff (ed.), *Advanced EPR*, Elsevier, Amsterdam (1989).
2. L. Kevan, M.K. Bowman (eds.), *Modern Pulsed and Continuous Wave Electron Spin Resonance*, Wiley, New York (1990).
3. A. Schweiger, *Angew. Chem.* **103**, 223–250 (1991); *Angew. Chem. Int. Ed. Engl.* **30**, 265–292 (1991).
4. H. Cho, S. Pfenninger, C. Gemperle, A. Schweiger and R.R. Ernst, *Chem. Phys. Lett.* **160**, 391–395 (1989).
5. C. Gemperle, A. Schweiger and R.R. Ernst, *Chem. Phys. Lett.* **178**, 565–572 (1991).
6. A. Schweiger, C. Gemperle and R.R. Ernst, *J. Magn. Reson.* **86**, 70–81 (1990).
7. E. Hustedt, A. Schweiger and R.R. Ernst, to be published.
8. A. Schweiger, in Ref.1, p.254.
9. E.J. Reijerse and S.A. Dikanov, *J. Chem. Phys.* **95**, 836–845 (1991).
10. C. Gemperle, G. Aebli, A. Schweiger and R.R. Ernst, *J. Magn. Reson.* **88**, 241–256 (1990).
11. G. Aebli, C. Gemperle, A. Schweiger and R.R. Ernst, to be published.
12. H. Cho, S. Pfenninger, J. Forrer and A. Schweiger, *Chem. Phys. Lett.* **180**, 198–206 (1991).
13. Th. Wacker and A. Schweiger, *Chem. Phys. Lett.*, in press.
14. Th. Wacker and A. Schweiger, to be published.
15. G. Sierra, A. Schweiger and R.R. Ernst, *Chem. Phys. Lett.*, in press.
16. G. Sierra, A. Schweiger and R.R. Ernst, to be published.
17. A. Schweiger, to be published.
18. A.V. Astashkin and A. Schweiger, *Chem. Phys. Lett.* **174**, 595–602 (1990).
19. J. Forrer, this conference.
20. R. Jakob, A. Schweiger and R.R. Ernst, to be published.

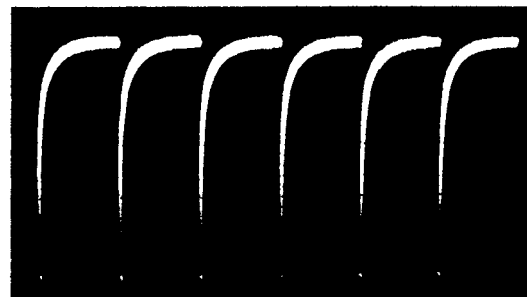


Fig.11: Oscilloscope photograph of inversion recovery signals. Time interval between the 180° pulses: 500 μ s.
Sample: single crystal of $Cu(sal)_2$.